B. Electrochem 4(5) May 1988, pp 497-504

ANODIC OXIDE AND ITS EFFECT ON THE PERFORMANCE OF n-InP PEC CELLS*

Y RAMPRAKASH
Central Electrochemical Research Institute, Karaikudi-623 006, INDIA
S BASU and D N BOSE
Materials Science Centre, Indian Institute of Technology, Kharagpur-721 302, INDIA

[Received: 1987 December; Accepted: 1988 March]

The effect of thin oxide films formed anodically on the surface of n-InP was investigated in redox photoelectrochemical cells. Studies relating to the I- V, C-V, spectral response and solar cell behaviour were carried out. In 0.1M NaOH-0.1M $K_4Fe(CN)_6$, -0.1M $K_3Fe(CN)_6$, J_0 and n showed a decrease in their value for oxidized electrodes compared with bare InP. Barrier heights derived from I-V and C-V data showed an increase with oxide. At $\lambda = 0.55 \mu$ m, the maximum value of the absolute quantum efficiency was 0.68 without oxide; 0.55 and 0.40 respectively with increasing oxide thickness. In 1M NaOH-1M K_4 Fe $(CN)_6$ - 1M K_3 $Fe(CN)_6$, the PEC cell showed $V_{oc} = 0.44$ V, $J_{sc} = 6.4$ mAcm^{-2} , FF = 0.43 with oxide, at 66 mW cm^{-2} tungsten-halogen illumination.

Key words: Indium phosphide, anodic oxide, photoelectrode, photoelectrochemical cell, solar energy conversion

INTRODUCTION

Oxide films can be grown on metals or semiconductor surfaces by anodization in a suitable electrolyte under potentiostatic or galvanostatic conditions. The anodic oxides on semiconductors find important application in the fabrication of Schottky-barrier devices. In the field of photoelectrochemistry, semiconductors prone to anodic dissolution can be protected by thin oxide films grown anodically over their surface. Another important application is, for determining Hall mobility and resistivity data of semiconductor substrates. It was shown [1] that carrier concentration profiles of InP implanted with S and Si can be obtained by anodically oxidizing the implanted layers and then determining the carrier concentration versus depth profiles of the implanted InP.

Indium phosphide is an attractive material for both solid state and liquid- junction solar cell applications because its bandgap (1.34 eV at 300K) is suitably matched to the solar spectrum. As a direct bandgap material, it has the lowest absorption depth viz. 0.3 μm [2] for visible radiation than any other known material for solar cells. Another important feature, which makes its choice against GaAs for solar energy conversion applications, is its low surface recombination velocity (10^3 cm sec^{-1}) compared to 10^7 cm sec^{-1} for GaAs [3]. In the studies on n-InP/NaOH-K_4 $Fe(CN)_6$ - K_3 $Fe(CN)_6$/Pt [4] it was observed that InP undergoes photocorrosion due to oxidation by photogenerated holes. The growth of an anodic oxide on InP and its characterization, has been reported in detail [1,5-15]. The role of oxide films in obtaining improved performance of Schottky barriers and liquid junction solar cells based on InP have been reported [8,16-17].

The results on the performance of InP photoelectrodes covered with thin anodic oxide layers for surface protection are reported in this paper.

EXPERIMENTAL

The single crystals of n-InP were obtained from M.C.P. (U.K.) and have the following specifications: $\rho = 0.027$ ohm cm^{-1}, n = 1.92×10^{17} cm^{-3} and μm = 1203 cm^2 V^{-1} sec^{-1}. The bandgap obtained from optical absorption studies was found to be 1.34 eV at room temperatue (300K).

The samples were initially cleaned ultrasonically in sequential baths of o- xylene, acetone and finally rinsed in methanol. Ohmic contact to the n-InP surface was provided by In metal alloyed to it at 673K in hydrogen atmosphere. The mechanically polished surface, was etched in 1% bromine-methanol mix ure for 20 seconds to obtain a shiny mirror like surface.

The photoelectrochemical studies on oxidized and unoxidized InP electrodes (area = 0.04 cm^2) were performed in 1M NaOH - 1M $K_4Fe(CN)_6$ - 1M K_3 $Fe(CN)_6$ or 0.1M NaOH-0.1M K_4 $Fe(CN)_6$ 0.1M K_3 $Fe(CN)_6$ at an illumination intensity of 66 mW cm^{-2} provided by a 1.5 KW tungsten-halogen lamp, the light from which was passed through a 2 cm circulating water filter, before focussing it on to the photoelectrode by a condensing lens.

Spectral response studies were done with the help of a Jarrel-Ash monochromator. The intensity of the monochromatic light was determined by a Si photodiode whose spectral responsivity (μA/ μW) is known.

Dark current-voltage (I-V) and capacitance-voltage (C-V) studies were conducted only for a 2-electrode cell configuration as the aim was only to investigate the Schottky barrier properties of the anodic oxide covered InP in an electrolyte. For the I-V studies, small d.c. potentials from a regulated power supply were applied across the cell. The capacitance was measured under increasing reverse bias with the help of a LCR balancing bridge. The a.c. signal applied was 25 mV peak-to-peak and the measurement frequency was 1KHz. In all the experiments, the voltages are generally measured by a high input impedance voltmeter and currents by a Keithley (160B) digital multimeter. The short-circuit current was measured as a voltage drop across a standard resistance of 1.1 ohm value.

---

* Part of Ph D work carried out during 1978-83

Oxide growth

The experimental technique for the anodization of InP was similar to the one previously reported by other workers [18]. The electrolyte was prepared by adding 3 g pf tartaric acid to 100 ml of triple distilled water, the pH of which was then adjusted to approximately 6 by adding 25% ammonia solution. 15 ml of the buffered solution was then added to 3.0 ml of propylene glycol to maintain a ratio of 1:2. Propylene-glycol-tartaric acid (PGT) electrolyte was chosen since it was found that reproducible oxide layers can be grown in this medium. It was also well established [18] that anodization in glycol and water (AGW) is superior in comparison to anodization in aqueous solutions (AAS), since the former facilitates growth of thicker oxide films and is insensitive to pH variations. Fig. 1 shows the experimental arrangement for anodization of InP.

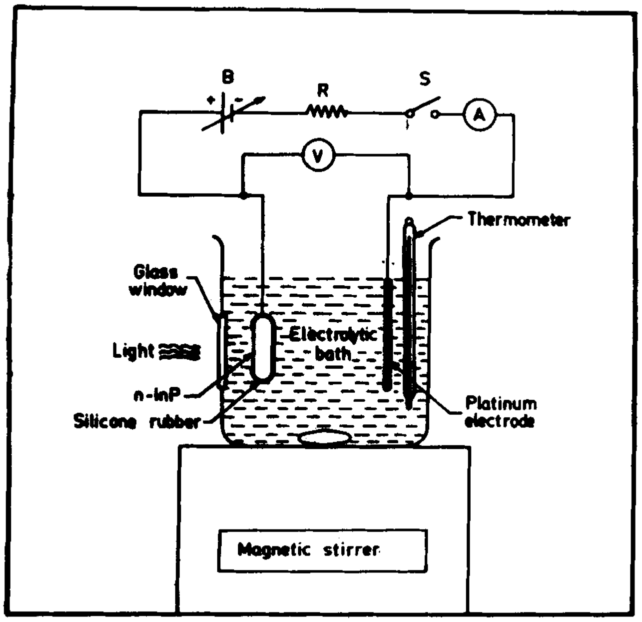

Fig. 1: Experimental arrangement for anodization of InP

A 50 ml beaker containing the bath was placed on a magnetic stirrer and moderately stirred at low speeds to ensure uniform growth of oxide during the anodization. Single crystal InP electrodes, mounted on teflon strips with the help of insulating epoxy, were placed sufficiently deep into the electrolyte to prevent current crowding near the regions of the anode which were very close to the cathode. A platinum foil was used as the counter electrode. The positive terminal of a constant power supply (B) (Fig.1) was connected to the n-InP electrode through a 1 megohm series resistance (R) and a milliammeter (A), while the negative terminal went to the Pt electrode. A switch (S) was provided to interrupt the curent whenever required. During anodization, the InP electrode was illuminated by a 200W tungsten lamp from a distance of 30 cm to provide additional holes required for oxide growth.

In the actual experiment, a constant voltage between 15-180V was applied to the InP electrode to set an initial current density of 3mA cm^{-2} . Although oxide layers can be grown, also at low current densities, less than 1 mA cm^{-2} [10], the high current densities were employed to facilitate growth of thicker oxide films. These are essential for adequate surface protection of n-InP in the highly corrosive electrolytes used in the present studies.

Fig. 2 shows a typical current-time plot for n-Inp anodized for 5 minutes at 175 V at an initial current of 120μA. The fast decrease in the current from the initial value indicated the formation of the oxide. The figure also shows that the current remained practically unchanged over the time interval 210 to 300 sec, due to growth saturation. The extent of dissolution of the oxide was not determined as it was reported [1] that the rate of dissolution viz. 1.7 x 10^{-2} A sec^{-1} was quite small compared to the oxide growth rate, which was typically 1 A sec^{-1} at pH 6 for initial current densities less than 1 mA cm^{-2}. Anodization was also performed for 2 and 10 minutes duration, at similar current densities. After the oxide growth, the samples were cleaned thoroughly in triple distilled water and dried under argon.

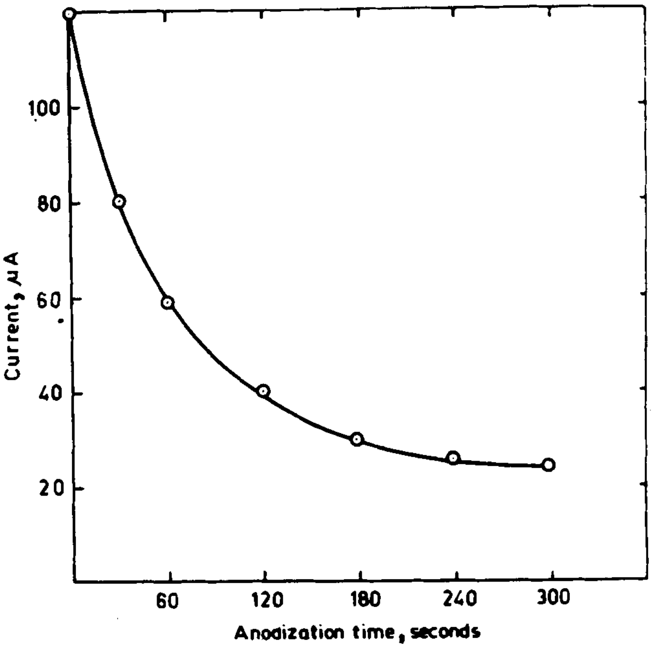

Fig. 2: Typical current-time plot during the oxide growth

The thickness of the oxide was determined by ellipsometry in which an ellipsometer (Model 80-2HP of Gartner Scientific Corporation, USA) was used. The values of Δ and ψ were measured at five different places on the oxide surface. The angle of incidence (ϕ_0) of the He-Ne laser beam was 70°. The refractive index of the oxide was assumed to be 1.9 which is the value for In_2O_3 [7]. From the same reference, the refractive index of InP was taken as 3.4.

The Auger studies were carried out with the help of a Physical Electronics Inc. thin film analyzer. The Auger lines of In, O and P were recorded as the surface was sputter etched. In terms of Ta_2O_5 sputter rate, a one minute sputtering of the oxide was equivalent to removal of 30 A° of the layer.

RESULTS AND DISCUSSION

Characterization of the anodic oxide

Resistivity

The resistivity of the oxide was determined by a two-probe technique and was found to be in the range of 7 to 8 x 10^8 ohm cm.

Thickness

The thicknesses of the oxide films as determined by ellipsometry, were 407 and 958 A° respectively for the samples anodized for 2 and 5 minutes. The thickness was also estimated from the colour of the oxide film and duration of oxide growth by comparing with earlier studies [1]. The thickness estimated in this way, was found to be approximately 400 and 1200 A respectively. For the sample anodized for 10 minutes, the thickness estimated was approximately 1800 A.

Composition analysis from Auger depth profiles

The Auger composition depth profiles for the oxide layers grown for 5 and 10 minutes are shown in Figs. 3 and 4. Although the peak heights of the elements cannot be used for quantitative analysis due to lack of data regarding the instrument sensitivities for different elements, it can be seen that peak heights of lines corresponding to oxygen in both the figures is relatively high compared to In and P lines. The anodic oxides grown by previous workers [14] also contained a very large amount of oxygen but the In and P peak heights were relatively small. Other workers [7] observed In peak height to be relatively high compared to oxygen, for a 1000 A° thick oxide, grown in a glycol-electrolyte medium for 10 minutes at an initial current density of 0.3 mA cm^{-2}. Their results are shown in the inset of Fig.4 which makes it clear that the PGT grown oxide does not contain an outer layer of constant composition, but is a mixture of $In_2O_3$and P_2O_5. By comparison, the present results also show that the oxide layers grown may also have an outer layer, which is a mixture of In_2O_3 and P_2O_5 .

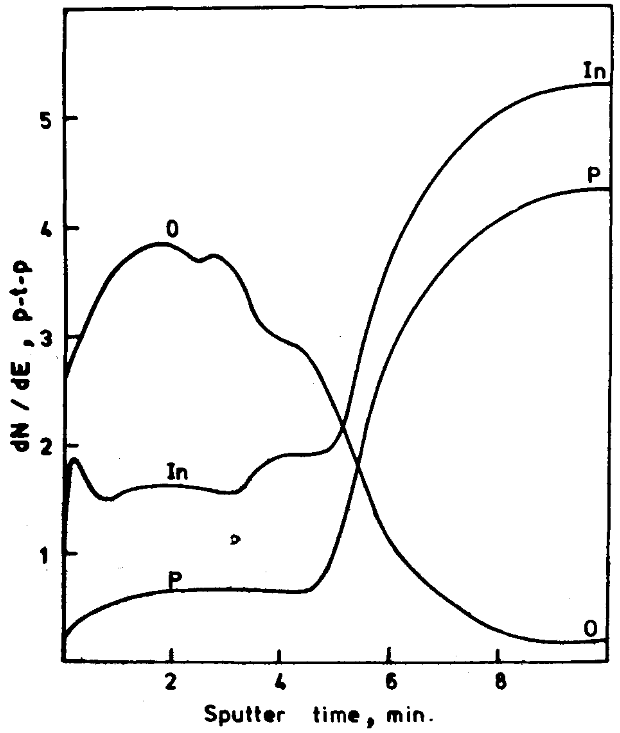

Fig.3: Auger-peak composition profile for an oxide grown for 5 minutes

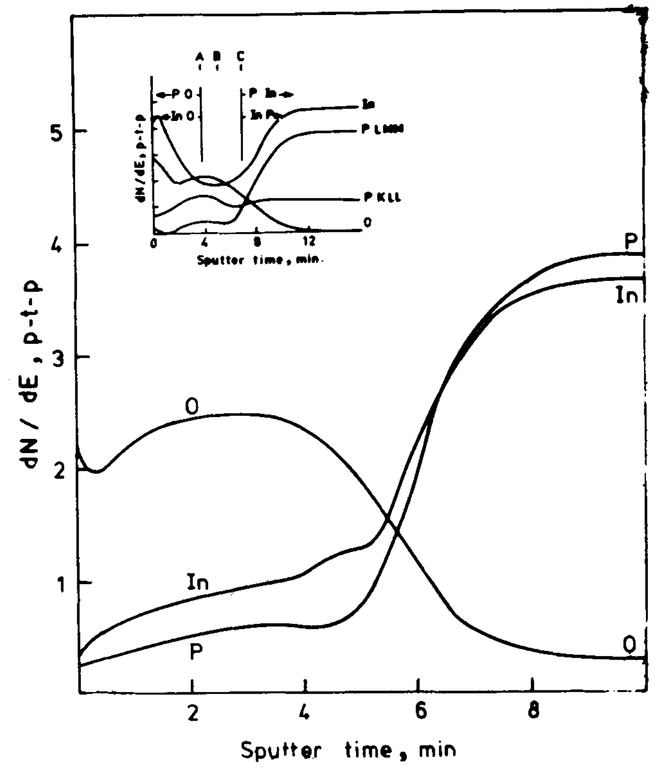

Fig.4: Auger-peak composition profile for an oxide grown for 10 minutes (Inset: after Wilmsen and Kee, ref. 7)

The transition from the In-O bonding to In-P bonding occurred over a region of 60 Å in width, in terms of Ta_2O_5 sputtering rate. Other workers [6] reported a transition width in the range 250-300 Å. The thickness of the oxide films in terms of equivalent Ta_2O_5 layer thickness were found to be 156 and 168 A respectively for the samples anodized for 5 and 10 minutes. It shows an evidence of an approach towards a terminal thickness of 170 A°. It seems a mixture of In-O, P-O and In-O bonding is highly probable within the transition region as reported [7].

Photoelectrochemical studies

J-V studies in dark

The dark J-V characteristics obtained under forward bias for n-InP electrodes covered with oxide films of thickness 407 and 958 A° are shown in Fig. 5 for two concentrations of the electrlyte. For comparison, the results obtained on unoxidized surfaces are also shown in the same figure. The forward dark current was found to have an exponential dependence with voltage according to:

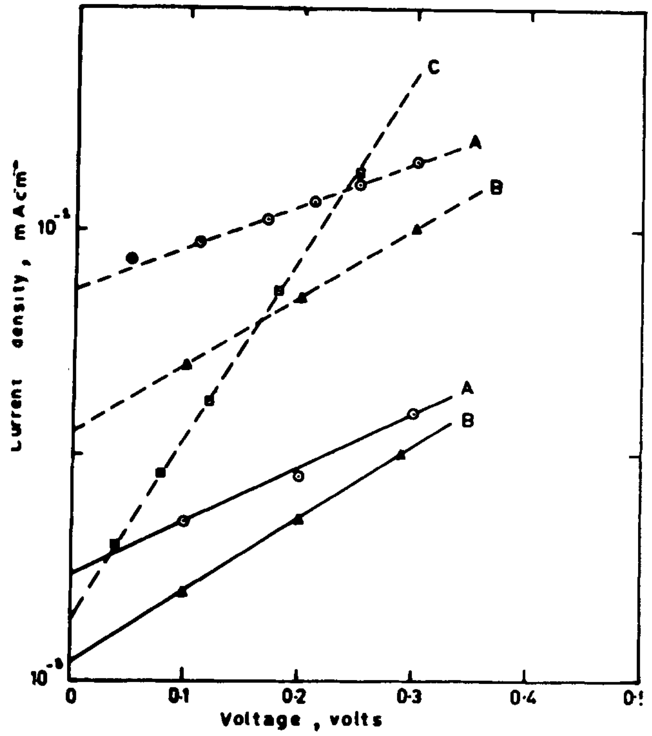

Fig.5: Log J vs V plot
Broken line: n-InP in 1M NaOH-1M $K_4Fe(CN)_6$ -1M $K_3Fe(CN)_6$
Full line: n-InP in 0.1M NaOH-0.1M $K_4Fe(CN)_6$ - 0.1M $K_3Fe(CN)_6$
A-Without oxide, B-With oxide, thickness = 407 A°
C-With oxide, thickness = 958 A°

TABLE-I: J_0 and n for bare and oxidized InP electrodes

Redox	Unoxidized		Oxidized			
	J A . cm⁻²	n	Thickness = 407 A°		Thickness = 958 A°	
			J A . cm⁻²	n	J A . cm⁻²	n
0.1M NaOH- 0.1M $K_4Fe(CN)_6$ 0.1M $K_3Fe(CN)_6$	2.9×10^{-6}	7.28	1.2×10^{-6}	5.47	-	-
1.0M NaOH - 1.0M$K_4Fe(CN)_6$- 1.0M$K_3Fe(CN)_6$	5.4×10^{-5}	9.16	1.2×10^{-5}	5.77	1.9×10^{-6}	2.15

$$J = J \left[\exp\left(\frac{qV}{nkT}\right) - 1\right] \quad \ldots (1)$$

where J_0 is the reverse saturation current density in A. cm⁻² and n the ideality factor, according to the Schottky barrier theory [19]. These values are summarized below:

It is clear, from Table I, that oxidized surfaces showed better J_0 and n values, although improvement was considerably good with thicker oxide films. The junction also exhibited improved rectification behaviour in 0.1M NaOH-0.1M $K_4Fe(CN)_6$ - 0.1M $K_3Fe(CN)_6$.

The above values of J_0 can be used to calculate the barrier height ϕ_{B_M} for InP according to :

$$J_0 = A^* T^2 \exp\left[-\frac{q\phi_{B_M}}{kT}\right] \quad \ldots (2)$$

The Richardson constant A* was found to have a value of 0.3 A cm⁻² K⁻¹ [20]. ϕ_{B_M} values obtained from eqn. 2 are tabulated below:

TABLE-II: Schottky-barrier heights for the n-InP/electrolyte contact

Redox	Oxide thickness A°	Barrier height ϕ_{B_M}, eV
0.1M NaOH - 0.1M $K_4Fe(CN)_6$- 0.1M $K_3Fe(CN)_6$	No oxide	0.57
	407	0.59
1M NaOH - 1M $K_4Fe(CN)_6$- 1M $K_3Fe(CN)_6$	No oxide	0.50
	407	0.54
	958	0.58

The small increase in barrier height on 0.1M NaOH-0.1M $K_4Fe(CN)_6$ - 0.1M $K_3Fe(CN)_6$ is a consequence of a small decrease in J_0 for the oxidized surface. However, a slightly larger increase in ϕ_{B_M} was observed in 1M NaOH-$K_4Fe(CN)_6$ -1M $K_3Fe(CN)_6$ for the same thickness of oxide. A more pronounced increase was observed with thicker oxide (Table II).

C-V studies

The C^{-2} vs V_{fb} variation is shown in Fig. 6. V was determined from the extrapolated intercept of the Mott-Schottky plot. N_D was calculated from the slope, assuming ε_s = 10.3 for InP. The barrier height was calculated from the voltage intercept using Schottky-barrier theory [19]. The results are summarized in Table III.

The increase in the flat-band potential on oxidized surfaces is due to increase in the band bending at the InP-electrolyte interface. Assuming no voltage drop in oxide, the applied voltage will mainly appear across the space charge layer in InP. The ionized donor densities, therefore, obtained from the Mott-Schottky slopes is an indication of the free electron density in n-InP.

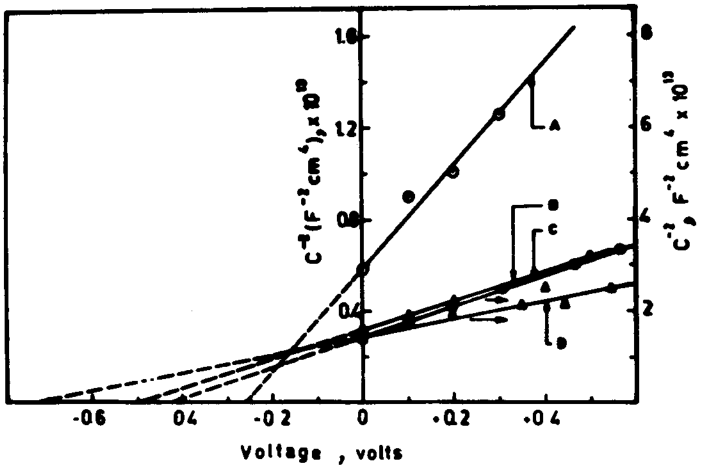

Fig.6: Mott-Schottky plot for n-InP at 1 KHz
0.1M NaOH-0.1M K_4 $Fe(CN)_6$ -0.1M K_3 $Fe(CN)_6$
A - Without oxide, B - With oxide, thickness = 958 A°
1M NaOH-1M $K_4Fe(CN)_6$ -1M $K_3Fe(CN)_6$
C - Without oxide, D - With oxide, thickness = 958 A°

TABLE-III: V_{fb}, ϕ_{Bm} and N_D values for the bare and oxide covered InP electrodes

Redox	Unoxidized			Oxidized (thickness = 958 Å)		
	V_{fb} V	ϕ_{Bm} eV	N_D cm^{-3}	V_{fb} V	ϕ_{Bm} eV	N_D cm^{-3}
0.1M NaOH- 0.1M $K_4Fe(CN)_6$ 0.1M $K_3Fe(CN)_6$	-0.26	0.36	$5x10^{17}$	-0.49	0.59	$1.8x10^{18}$
1M NaOH - 1N $K_4Fe(CN)_6$- 1N $K_3Fe(CN)_6$	-0.40	0.50	$3.3x10^{17}$	0.72	0.82	$5.7x10^{17}$

Spectral response

The spectral dependence of the absolute quantum efficiencies (Q.E.) for the oxide covered photoelectrode is shown in Fig.7. The maximum quantum efficiencies viz. 0.55 and 0.40, occurring at $\lambda = 0.55 \mu m$, indicated that thicker oxide films greatly reduce the cell efficiency due to increased carrier scattering and recombination losses. The nature of the curves differed greatly for the two oxide thicknesses studied here. With the thinner oxide (curve a), the response was flat over the wavelength region 0.5 to 0.8 μm, while an increase and then a decrease in the Q.E. was observed with the thicker oxide film (curve b). However, the curves (a) and (b) showed a similar trend to decrease beyond $\lambda = 0.8 \mu m$ (not shown in Fig.) meets the wavelength axis at 0.96 μm which is close to the cut off = 0.925 μm for InP.

A comparison of the spectral response curves for the oxidized with the unoxidized electrodes (curve c, Fig.7) showed that quantum efficiencies were high for the latter. Further it may be noted that the maximum quantum efficiency was 0.68 at $\lambda = 0.55 \mu m$ which reduced to 0.40 for an oxidized (oxide thickness = 958 A°) electrode. The decrease in quantum efficiency with oxide can be explained in terms of losses due to trapping and recombination, that occur during carrier transport across the oxide whose thickness is greater than the tunneling width for electrons (40 Å). It was shown [20] that an anodic oxide of 40 A° greatly improved the performance of MOS diodes fabricated on InP. The spectral response of these diodes was flat and exhibited 60% collection efficiencies over the visible region due to low surface recombination velocity.

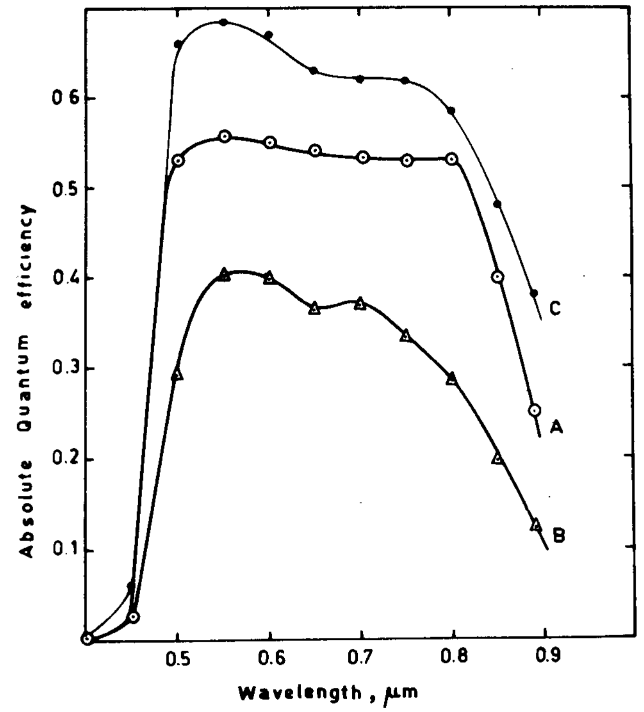

Fig.7: Spectral dependence of absolute quantum efficiency for n-InP in 1M NaOH-1M $K_4Fe(CN)_6$ -1M $K_3Fe(CN)_6$
A - With oxide, thickness = 958 A°
B - With oxide, thickness = 1800 A°; and
C - Without oxide

Solar cell characteristics

The power output curves (Fig.8) were obtained for the bare and oxide covered InP in 1M NaOH-1M $K_4Fe(CN)_6$ - 1M K_3 $Fe(CN)_6$ solutions under 66 mW cm^{-2} tungsten-halogen illumination. The parameters V_{oc}, J_{sc} FF and η obtained from these curves are summarized in Table IV.

The increase in V_{oc} was less than expected considering the shift in the V_{fb} from -0.40 to -0.72 for the 958 A° oxide. Although less, the increase in V_{oc} may arise due to the trapping of negative charge within the oxide film or at the surface of InP. This negative

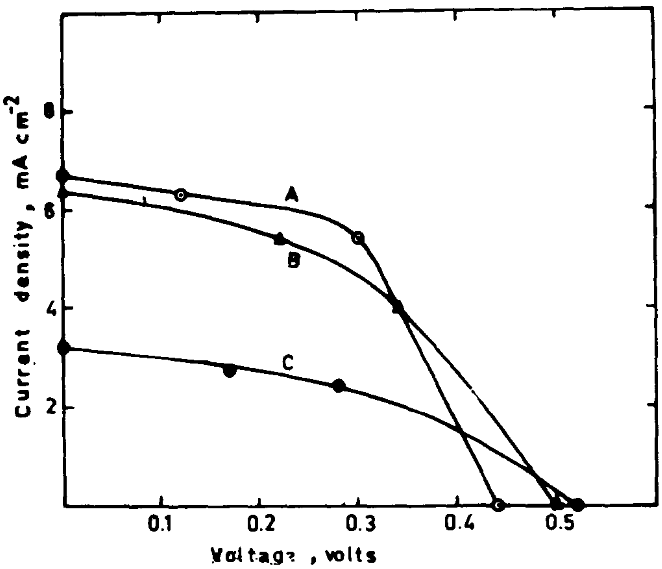

Fig.8 Power output characteristics in 1M NaOH-1M K_4 Fe(CN)$_6$ - 1M K_3Fe(CN)$_6$ at 66mw cm^{-2} tungsten-halogen illumination
A- Unoxidized surface
B- With oxide, thickness = 958 A°
C- With oxide, thickenss ~ 1800 A°

TABLE-IV: Parameters of power output for the bare and oxidized InP photoelectrodes

	V_{oc} (V)	J_{sc} (mA cm^{-2})	FF	η (%)
Unoxidized	0.44	6.70	0.55	2.4
Oxide covered				
958 A°	0.50	6.40	0.43	2.0
1800 A°	0.52	3.20	0.42	1.0

charge will cause an increase in the positive space charge within the depletion layer region and thereby increase the band bending. The low photocurrents obtained with oxide covered electrodes are generally due to poor hole transport across it.

Intensity dependence of J_{sc} and V_{oc}

The light intensity (IL) dependence of J_{sc} is shown in Fig. 9. The short-circuit current density varied linearly with I_L but exhibited a slope of 0.73 and 0.74 respectively for the unoxidized and oxidized (958 A°) electrodes. The deviation from a slope of unity might be due to poor carrier collection at high intensities.

V_{oc} variation with log I_L is shown in Fig.10. The slope of the plot in the logarithmic region is given by :

$$\frac{dV_{oc}}{d \log I_L} = -2.3 \frac{nKT}{q} \qquad \dots (3)$$

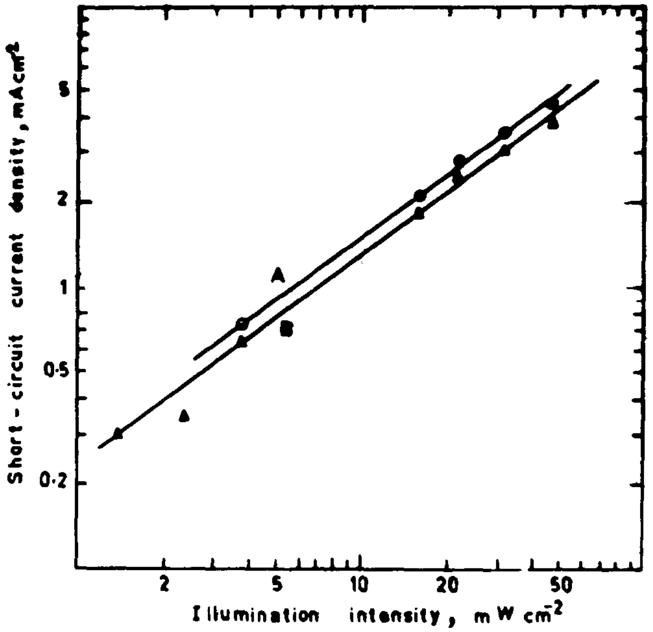

Fig.9: J_{sc} vs log I_L plot in 1M NaOH-1M K_4Fe(CN)$_6$-1MK_3Fe(CN)$_6$ A-Without oxide, B-With oxide, thickness = 958 A°

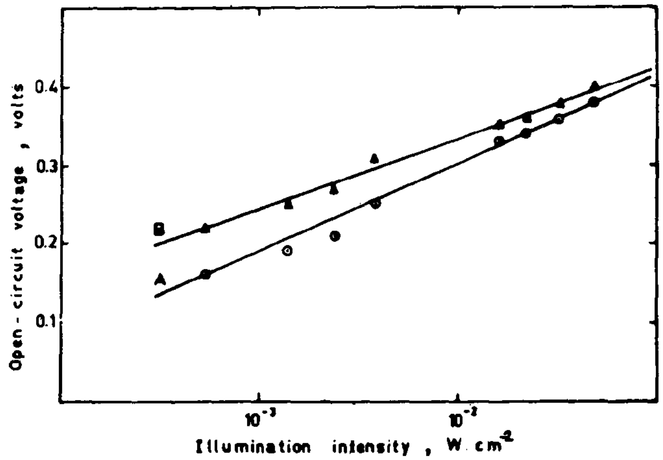

Fig.10: V vs log I_L plot in 1M NaOH-1M K_4 Fe (CN)$_6$ -1M K_3 Fe(CN)$_6$, A-Without oxide, B-With oxide, thickness = 958 A°

The slopes were found to be 0.11 ad 0.09 respectively for the bare and the oxide covered (958 A°) electrodes. Similar values have been reported [21] on TiO_2 PEC cells. For $n = 1$, eq. (3) gives a slope of 0.06 V. Using the values of [$dV_{oc}/d \log I_L$] as determined above, n values were calculated and found to be 1.91 and 1.63 respectively for the two electrodes. The corresponding values determined from dark I-V curves (Fig. 5) were 9.16 and 2.15 respectively. One of the important explanations for the occurrence of high n factors in semiconductor-electrolyte junctions is the presence of a high density of surface states and the variation of their charge with applied potential, thus resulting in a substantial voltage drop across the Helmholtz's double layer [22]. An insulating film at the semiconductor surface also can increase the n-factor [23].

The variation of J_{sc} and V_{oc} with I_L can be fitted to an equation of the form:

$$J_{sc} = J_o \left[\exp\left(\frac{qV_{oc}}{nKT}\right) - 1\right] \qquad \ldots (4)$$

Fig.11 shows the variation of J_{sc} with V_{oc} for different intensities of illumination. J_o obtained from extrapolating the straight line to $V_{oc} = 0$ was found to be 2.8×10^{-5} and 2.5×10^{-6} A cm^{-2} respectively for the bare and oxidized electrode. Correspondingly, the n factor decreased from 3.03 to 3.18. Comparing these values with n obtained from dark J-V plots (Fig. 5), it can be observed that there is reduction in n from 9.17 (Table I) to 3.03 (Fig. 11) for the unoxidized electrode. This shows that illumination brings in a saturation of the active surface traps responsible for generation-recombination processes, thus allowing direct charge transfer to occur from the filled levels of the valence band of the semiconductor to the unfilled levels in the electrolyte, with negligible contribution from the surface states. On the other hand, the density of surface states would normally be reduced for the oxidized InP due to surface passivation. Therefore, irrespective of whether the electrode was in dark or illuminated, the density of surface states should remain the same, provided dissolution of oxide does not occur in the electrolyte. This is reflected in the n value, which did not vary in the two cases.

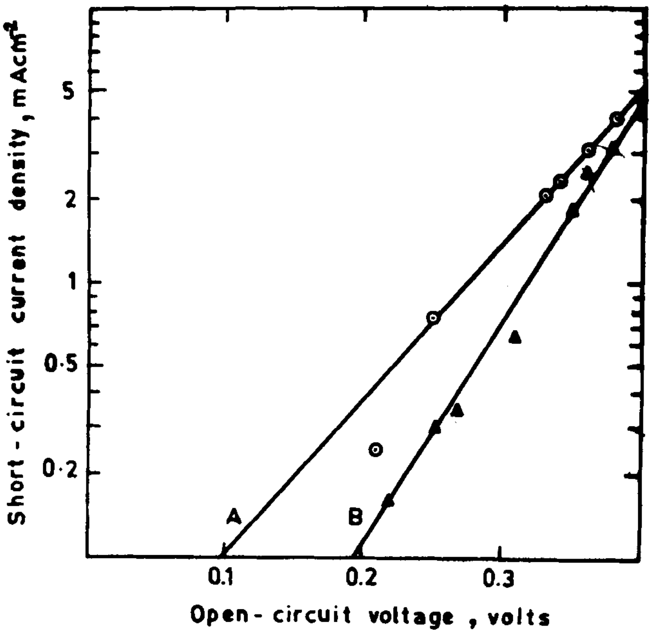

Fig.11: Log J_{sc} vs V_{oc} plot in 1M NaOH-1M $K_4 Fe (CN)_6$ -1M $K_3 Fe (CN)_6$
A- Without oxide, B- With oxide, thickness = 958 A°

Stability

The stability of the photoelectrode as determined by the constancy of the photocurrent was found to be 12 and 8 hours respectively for the oxide covered (958 A°) and bare InP photoelectrodes. In the former case, the photocurrent remained constant at 4 mA cm^{-2} for 12 hours and then decreased to 2 mA cm^{-2} during the next 12 hours. A thick white film covering the entire area of the photoelectrode was observed. Although anodic dissolution of In_2O_3 is contrary to expectation, the porous nature of the oxide film does not rule out the possibility of InP coming direct in contact with the electrolyte, ultimately leading to its dissolution. Auger analysis of the oxide revealed the presence of both In_2O_3 and P_2O_5 phases. The latter is a strong dehydrating agent and readily reacts with water. This might also be another possible reason for the observed dissolution.

CONCLUSIONS

Anodic oxide on n-InP improved the dark J-V characteristics by reducing J_o and n. Capacitance measurements showed increase in V_{fb} and barrier height. Spectral response studies showed reduction in absolute quantum efficiencies with oxide. The power output curves showed loss in photocurrent collection due to poor hole transport across the oxide. Photocurrent stability tests confirmed dissolution of InP.

Acknowledgement: Y R P is indebted to Dr. R P Rao and Dr. K R Murali for their help in spectral response measurements.

REFERENCES

1. J P Lorenzo, D E Davies and T C Ryan, *J Electrochem Soc,* **126** (1979) 118

2. R C Neville, *Solar Energy Conversion - The Solar Cell,* Elsevier Scientific Publishing Co., Amsterdam, 1978, p 128

3. H C Cassey, Jr and E Buehler, *Appl Phys Lett,* **30** (1977) 247

4. Y Ramprakash, S Basu and D N Bose, *J Indian Chem Soc,* **58** (1981) 153

5. C W Wilmsen, *Crit Rev Solid State Sci,* **5** (1975) 313

6. D L Lile and D L Collins, *Appl Phys Lett,* **28** (1976) 554

7. C W Wilmsen and R W Kee, (a) *J Vac Sci Technol,* **14** (1977) 953; (b) *Thin Solid Films,* **51** (1978) 93

8. O Wada and A Majerfeld, *Electronic Lett,* **14** (1978) 125

9. O Williams and J Wright, *J Mat Sci,* **13** (1978) 2292

10. T Ota and Y Horikoshi, *Jpn J Appl Phys,* **18** (1979) 989

11. K M Geib and C W Wilmsen, *J Vac Sci Technol,* **17** (1980) 952

12. D H Laughlin and C W Wilmsen, *Appl Phys Lett,* **37** (1980) 915

13. D De Cogan, G Eftekhari and B Tuck, *Thin Solid Films,* **91** (1982) 277 ,

14. M Salvi, P N Favennec, H L Haridon and C P Polous, *Thin Solid Films,* **87** (1982) 13

15. G Eftekhari,D De Cogan and B Tuck, *Phys Stat Sol,* **76** (1983) 331

16. A Heller, B Miller and F A Thiel, *Appl Phys Lett,* **38** (1981) 281

17. S Menezes, H J Lewerenz, F A Thiel and K J Bachmann, *Appl Phys Lett,* **38** (1981) 710

18. H Hasegewa and H L Hartnagel, *J Electrochem Soc,* **123** (1976) 713

19. S M Sze, *Physics of Semiconductor Devices,* Wiley Eastern Limited, New Delhi, (1979) p 394

20. K P Pande (Private communication)

21. W Gissler, P L Lensi and S Pizzini, *J Appl Electrochem,* **6** (1976) 9

22. B Vainas, G Hodes and J Du Bow, *J Electronal Chem,* **130** (1981) 391

23. W P Gomes and F Cardon, *Semiconductor liquid-junction solar cells,* Ed. A Heller, Proceedings Vol. 77-3, The Electrochemical Society Inc., Princeton, N J., 1977, p 120